MATCHED-PEAK INVERSION IN OCEAN ACOUSTIC TRAVEL-TIME TOMOGRAPHY

PACS REFERENCE: 43.30.Pc

Skarsoulis Emmanuel K.,
Institute of Applied and Computational Mathematics,
Foundation for Research and Technology Hellas,
P.O. Box 1527, GR-71110 Heraklion, GREECE
Tel: +30-810-391776,
Fax: +30-810-391801,
E-mail: eskars@iacm.forth.gr

ABSTRACT

Ocean acoustic travel-time tomography is a remote-sensing technique for monitoring the ocean interior using low-frequency sound waves. Tomographic inversions are usually linear, assuming perturbations about a fixed background state, and apply to identified travel-time data. An alternative inversion method is proposed here that can be applied to unidentified travel-time data. This method is based on peak matching and consists in finding those model states that best represent the observed arrival times. The matched-peak approach allows for multiple background states and thus for non-linear inversion, whereas it provides a weak solution to the identification problem.

INTRODUCTION

Ocean acoustic travel-time tomography was introduced by Munk and Wunsch [1], [2] as a remote-sensing technique for monitoring the ocean interior. Measuring the travel times of pulsed acoustic signals propagating through the water mass over a multitude of different paths, and exploiting the knowledge about how travel times are affected by the sound-speed (temperature) distribution in the water, the latter can be obtained by inversion. Inversions in ocean acoustic tomography are usually linear, solving for perturbations about an a priori known background state, and apply to identified travel-time data, i.e. to a subset of the observed peaks that have been associated with particular model peaks. The common way to establish this association is by first tracking the observed peaks, over a sequence of receptions, and then associating the observed tracks with model peaks.

An approach for the inversion of unidentified travel-time data has been recently developed [3]. Using the linearized model relations about a set of background states, arrival times and associated errors are calculated on a fine grid of model states discretizing the sound-speed parameter space. The consideration of a set of background states allows for the treatment of non-linear model relations. Each model state can explain a number of observed peaks in a reception lying within the uncertainty intervals of the corresponding predicted arrival times. The model states that identify the maximum number of observed peaks, described in terms of mean values and variances, provide a statistical answer (matched-peak solution) to the inversion problem. With this approach each tomographic reception can be treated independently, i.e. no

constraints are posed from previous-reception identification or inversion results. Accordingly, there is no need for initialization of the inversion procedure and, furthermore, discontinuous travel-time data can be treated.

The matched-peak approach provides, together with the solution of the inversion problem, a simultaneous weak solution to the identification problem. Besides the absolute-time and relative-time inversion problems the matched-peak approach can be applied to solve problems of non-linear clock-drift correction, offset calibration and drifting source navigation. It has been used for the analysis of travel-time data from long-term tomography measurements in the Mediterranean [3], [4] and in the Labrador sea [5]. A description of the matched-peak approach is presented below together with some application results.

THE MATCHED-PEAK APPROACH

The solution of the forward problem in ocean acoustic travel-time tomography leads to a set of model relations

$$\boldsymbol{t}_i = g_i(\vec{\boldsymbol{J}}), \quad i = 1,\ldots,I, \quad \vec{\boldsymbol{J}} \in \Theta, \tag{1}$$

non-linear in general, between the sound-speed parameter vector $\vec{\boldsymbol{J}} = (\boldsymbol{J}_1,\ldots,\boldsymbol{J}_L)$ and the arrival times $\boldsymbol{t}_i$, $i = 1,\ldots,I$; $\vec{\boldsymbol{J}}$ belongs to the parameter space Θ. Arrival times can be defined in various ways using the notions of ray, modal or peak arrivals [2], [6]. The selection of the one or the other approach relies on the ability to resolve the particular model observables in the measured arrival patterns. Linearizing the relations (1) about a set of background states $\vec{\boldsymbol{J}}^{(b)}$, $b \in \mathrm{B}$, with corresponding arrival times $\boldsymbol{t}_i^{(b)} = g_i(\vec{\boldsymbol{J}}^{(b)})$, and, further, discretizing the local parameter space, about each background state, into a local grid with index $k \in K$, the following relations can be obtained

$$\tilde{\boldsymbol{t}}_i(b,k) = \boldsymbol{t}_i^{(b)} + \sum_{l=1}^{L} \frac{\partial g_i(\vec{\boldsymbol{J}}^{(b)})}{\partial \boldsymbol{J}_l} [\tilde{\boldsymbol{J}}_l(b,k) - \boldsymbol{J}_l^{(b)}], \quad i = 1,\ldots,I, \quad b \in \mathrm{B}, \quad k \in K, \tag{2}$$

where $\{\tilde{\boldsymbol{J}}_l(b,k)\}$ represent the discrete model states, and $\{\tilde{\boldsymbol{t}}_i(b,k)\}$ the corresponding arrival times. Using the relations (2) the arrival times corresponding to a set of discrete model states spanning the parameter space Θ can be calculated rapidly, since the full arrival-pattern calculations need to be carried out at a limited number of background model states $\vec{\boldsymbol{J}}^{(b)}$, $b \in \mathrm{B}$; the derivatives $\partial g_i(\vec{\boldsymbol{J}}^{(b)})/\partial \boldsymbol{J}_l$, called influence coefficients, can be expressed and calculated in terms of background quantities and sound-speed modes [2], [6]. Depending on the background state b and the size of the discretization $\boldsymbol{d}\vec{\boldsymbol{J}}$, an estimate for the upper-bound of the prediction error $\boldsymbol{e}_i(b, \boldsymbol{d}\vec{\boldsymbol{J}})$ can be obtained as a sum of a discretization error and an observation/modelling error n_i

$$\boldsymbol{e}_i(b, \boldsymbol{d}\vec{\boldsymbol{J}}) = \frac{1}{2} \sum_{l=1}^{L} \left| \frac{\partial g_i(\vec{\boldsymbol{J}}^{(b)})}{\partial \boldsymbol{J}_l} \boldsymbol{d}\boldsymbol{J}_l \right| + n_i, \quad i = 1,\ldots,I, \quad b \in \mathrm{B}, \tag{3}$$

The observed arrival times $\boldsymbol{t}_j^{(o)}$, $j = 1,\ldots,J$ are allowed to associate with the model arrival times $\tilde{\boldsymbol{t}}_i(b,k)$ if their time difference is smaller than the tolerance $\boldsymbol{e}_i(b, \boldsymbol{d}\vec{\boldsymbol{J}})$. Further, according to the peak matching principle, those model states are selected which maximize the number of associations between observed and model peaks.

Besides the ocean variability characterized by the model state $\{\tilde{J}_l(b,k)\}$ there are also other sources of variability such as such as mooring motion and clock drift. Taking into account these factors the model relations can be written in the following linearized form

$$\tilde{t}_i(b,k;dr,dt) = t_i^{(b)} + \sum_{l=1}^{L} \frac{\partial g_i(\vec{J}^{(b)})}{\partial J_l}[\tilde{J}_l(b,k) - J_l^{(b)}] + \frac{\partial t_i}{\partial r} dr + dt \qquad (4)$$

where dr stands for the range variation due to mooring motion and dt is the differential clock drift between source and receiver. Both dr and dt are functions of time. The common practice is that these quantities are estimated from additional navigation and clock-calibration data, and their effect is removed from the observed travel times prior to the analysis. There are cases, however, where they cannot be corrected for, due to lack of additional data [4], [5]. In such cases the matched-peak approach can be used to estimate these quantities together with the ocean state, by maximizing the number of peak associations as a function of the model state (b,k), the range variation dr and the differential clock drift dt. If there are several sections having a particular unknown in common, simultaneous transmissions along the sections can be exploited to obtain better estimates; in that case the quantity to maximize is the joint number of peak associations along all sections [4].

APPLICATION

The matched-peak approach is applied to travel-time data from the Thetis-2 experiment conducted from January to October 1994 in the western Mediterranean sea [7]. The Thetis-2 tomographic array, shown in Fig. 1, contained seven moored transceivers deployed at a nominal depth of 150 m. An HLF-5 source, marked by H in Fig. 1, of central frequency 250 Hz and effective bandwidth 62.5 Hz, insonified the basin at 8-hour intervals. The remaining 6 sources (W1-W5 and S), transmitting six times per day, were of Webb type with central frequency 400 Hz and effective bandwidth 100 Hz. The receivers at W1-W5 were modified to listen to both the 400-Hz and 250-Hz signals. Due to a leakage in the receiver part of W4 no navigation nor receiver data were available at W4. Accordingly, there are no receptions at W4 from the distant sources. Furthermore, the effect of the motions of W4 is present in all receptions of the W4 source at the distant receivers and cannot be removed prior to the analysis.

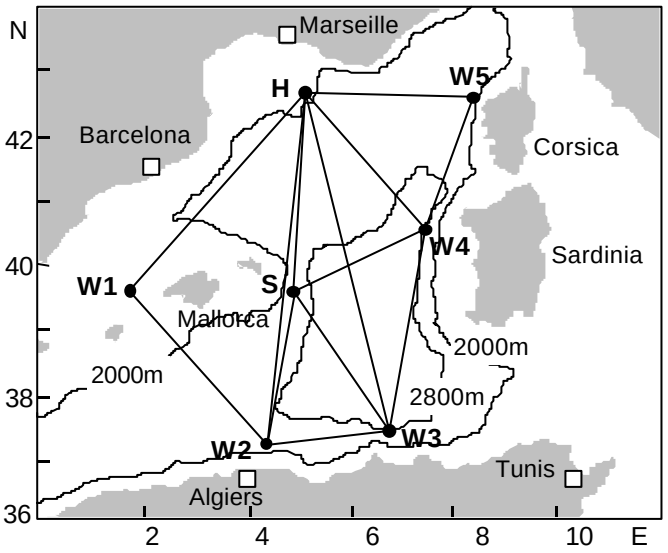

Figure 1. The geometry of the Thetis-2 experiment

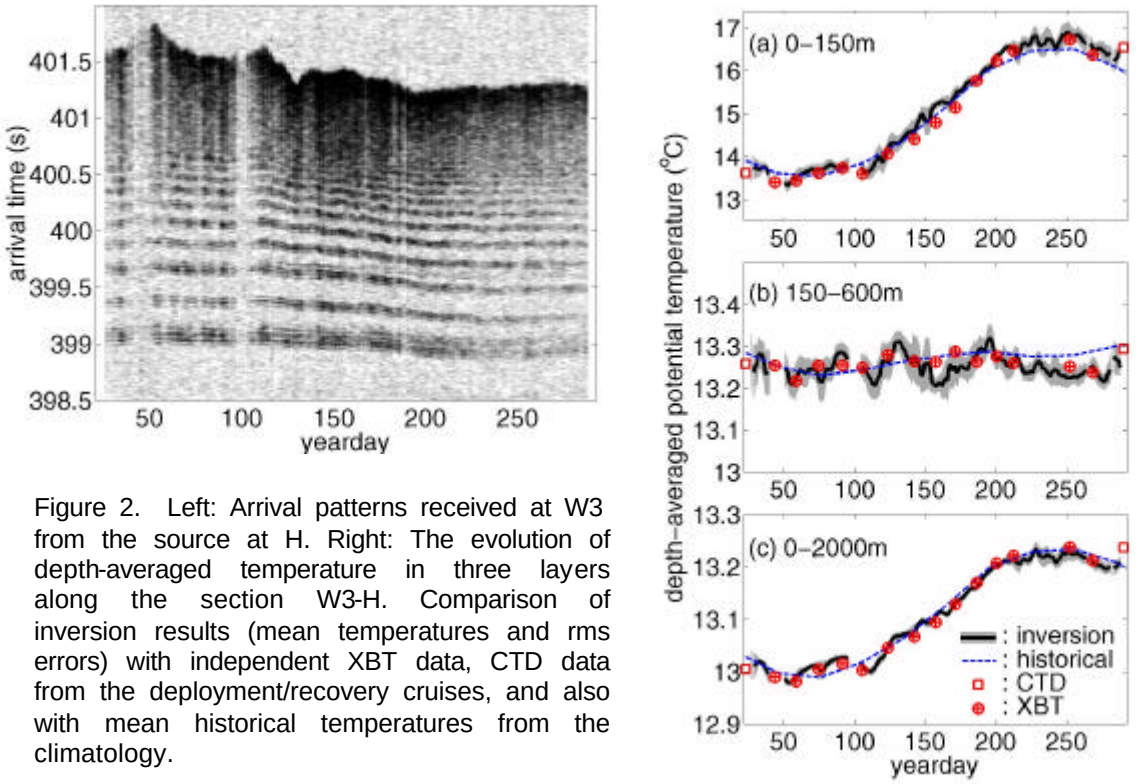

Figure 2. Left: Arrival patterns received at W3 from the source at H. Right: The evolution of depth-averaged temperature in three layers along the section W3-H. Comparison of inversion results (mean temperatures and rms errors) with independent XBT data, CTD data from the deployment/recovery cruises, and also with mean historical temperatures from the climatology.

The left-hand panel of Fig. 2 shows the acoustic receptions at W3 from the source at H (source-receiver range 604.7 km) over the 9month period covered by the experiment, after correlation (matched-filter) processing, clock-drift correction, mooring-motion correction and offset calibration. The horizontal axis of this figure represents yeardays of 1994 and spans the period of the experiment, whereas the vertical axis measures arrival time in seconds. A number of arrival groups can be distinguished in the first half of most receptions. These groups can be associated with particular groups of rays with steep propagation angles. Late arrivals are difficult to interpret in terms of ray arrivals because ray groups overlap with each other in this interval. To exploit the maximum of information contained in the intermediate and late part of the arrival patterns the peak-arrival approach [6] has been used, combined with normal-mode propagation modelling.

The panel on the right of Fig. 2 shows matched-peak inversion results for the section W3-H in the form of depth-averaged temperatures over three layers. Along the particular section a systematic XBT survey was conducted for verification purposes, parallel to the acoustic transmissions; the XBT line was occupied every two weeks using a commercial vessel connecting Marseille (France) to Skikda (Algeria). The XBT data and also the CTD data from the deployment and recovery cruises are shown in Fig. 11 as crossed circles and squares, respectively. Finally, the dashed lines in Fig. 11 represent the historical mean temperatures for each day of the year. It is seen that the gross seasonal changes are limited in the surface layer (0-150 m). The observed variability in the intermediate layer, below 150m, is mainly due to mesoscale activi ty. The surface layer also determines the evolution of the heat content over the entire water column, represented by the 02000m layer. The recovered mean temperatures give a satisfactory description of the actual conditions, the XBT/CTD data lying in most cases within the estimated error limits. A comparison of the inversions with the climatological data shows that there are deviations from the climatological mean conditions in all three layers and this is also confirmed by the XBT data. The amplitude of the seasonal signal in the surface layer is about 20% larger in the observations than in the historical data.

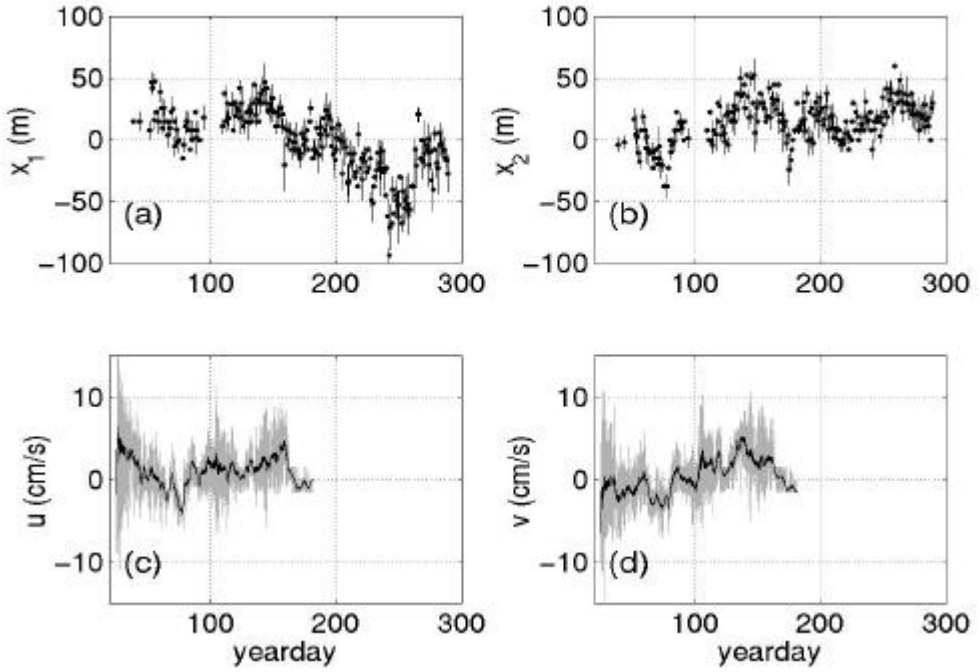

Figure 3. Upper panels: Estimated east-west (a) and north-south (b) displacement of the source at W4 and the corresponding rms errors. Lower panels: Eastward (c) and northward (d) current velocities measured on the mooring W4 at a depth of 351 m. The fluctuations in the actual measurements (gray lines) point to inertial currents. The black lines are the smoothed current velocities resulting from a moving average.

Besides the temperature inversions the matched-peak approach can be applied for the solution of the navigation and offset calibration problems. These problems arose in the case of the transceiver at W4 due to the lack of additional navigation data. The simultaneous receptions of the source W4 at H, W5, S and W3 were exploited to estimate the position of the central transceiver, the ocean state and the constant offset along each section [4]. The navigation results, and in particular the horizontal displacement of the source at W4 estimated from the multi-section matched-peak approach, are shown in the upper two panels (a and b) of Fig. 3: X_1 and X_2 are the east-west (positive east) and north-south (positive north) deviations of the source W4, respectively. The temporal coherence of the estimated displacements is important considering the fact that subsequent receptions have been analyzed independently of each other. The two lower panels of Fig. 3 show current velocities measured from a current meter mounted on the mooring W4 at 351 m depth. Even though the current measurements are 200 m deeper than the tomographic source there is a remarkable correlation between the evolution of current velocities and the estimated source displacements.

Fig. 4 presents inversion results for the entire tomographic array in the form of monthly-mean depth-averaged temperatures over the surface layer (0-150 m) and the intermediate layer (150-600 m). In the surface layer some anticipated features are observed, such as the warming trend from north to south (more precisely from northwest to southeast) and also the seasonal warming-cooling behaviour. In the intermediate layer a different pattern of spatial temperature distribution is observed, according to which the higher temperatures concentrate in the eastern part of the array. This distribution pattern is related with the presence of Levantine Intermediate Water or LIW (warm and salty water masses originating from the eastern Mediterranean) at intermediate depths in the eastern part of the basin, close to Corsica and Sardinia. Large part of the temperature variability observed in the intermediate layer is due to the detachment of LIW eddies and lenses from the eastern boundary.

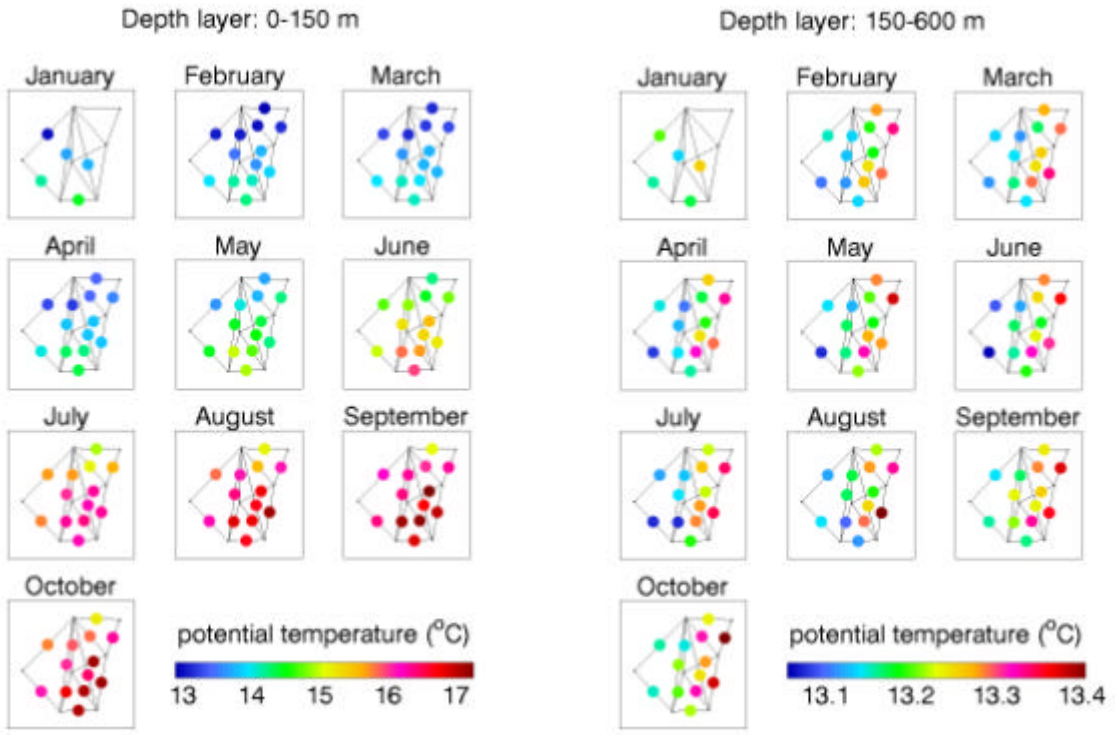

Figure 4. Matched-peak inversion results along the 13 sections of the Thetis-2 experiment: depth-averaged monthly mean temperatures in the surface layer (0-150 m) and the intermediate layer (150-600 m).

SUMMARY

The matched-peak inversion approach was briefly described and applied for the analysis of 9-month long travel-time data from the Thetis-2 experiment. This approach allowed for the automatic analysis of travel-time data from all 13 tomography sections without requiring the identification problem to be solved beforehand. Furthermore it was applied for the navigation of the mooring W4. The matched-peak approach treats each reception independently, such that there is no need for initialization data, whereas it can be applied to discontinuous travel-time data.

REFERENCES

[1] W.H. Munk and C. Wunsch, Ocean acoustic tomography: A scheme for large scale monitoring, Deep-Sea Res., Vol. 26A, pp. 123-161, 1979.
[2] W.H. Munk, P.F. Worcester and C. Wunsch, Ocean acoustic tomography, Cambridge Univ. Press, New York, 1995.
[3] E.K. Skarsoulis, A matched-peak inversion approach for ocean acoustic travel-time tomography, J. Acoust. Soc. Am., Vol. 107, pp. 1324-1332, 2000.
[4] E.K. Skarsoulis, Multi-section matched-peak tomographic inversion with a moving source, J. Acoust. Soc. Am., Vol. 110, pp. 786-797, 2001.
[5] D. Kindler, U. Send and E.K. Skarsoulis, Relative-time inversions in the Labrador Sea acoustic tomography experiment, Acta Acustica, Vol. 87, pp. 738-747, 2001.
[6] Athanassoulis, G.A. and Skarsoulis, E.K., Arrival-time perturbations of broadband tomographic signals due to sound-speed disturbances. A wave-theoretic approach, *J. Acoust. Soc. Am*, Vol. 97, pp. 3575-3588, 1995.
[7] Send, U. *et al*., Acoustic observations of heat content across the Mediterranean Sea, *Nature*, Vol. 385, pp. 615-617, 1997.